Original article

Osman Kireç, İhsan Alacabey, Kadir Erol* and Hüseyin Alkan

Removal of 17β-estradiol from aqueous systems with hydrophobic microspheres

https://doi.org/10.1515/polyeng-2020-0150
Received June 9, 2020; accepted December 22, 2020;
published online February 9, 2021

Abstract: Sub-microparticles have many applications in different fields today. In this study, it is aimed to develop hydrophobic microparticles as an alternative to existing methods and to determine the 17β-estradiol adsorption performance of this adsorbent to purify the 17β-estradiol hormone which is found as an endocrine disruptor in environmental waters with high capacity and low cost. In this study, L-phenylalanine containing Poly(HEMA-MAPA) microparticles were synthesized by microemulsion polymerization and used as adsorbent. Microparticles were characterized by Fourier transform infrared spectroscopy (FT-IR) and scanning electron microscope (SEM) methods. The size of the Poly(HEMA-MAPA) microparticles used was measured as 120–200 nm. Specific surface area and elemental analysis studies were also conducted. While the surface area of the particles was found to be a very high value of 1890 m^2/g, the amount of incorporation of MAPA into the polymeric structure was calculated as 0.43 mmol/g. Adsorption studies were carried out in the batch system under different ambient conditions (17β-estradiol concentration, temperature, ionic intensity). The adsorption capacity of Poly(HEMA-MAPA) microparticles was calculated to be 98.4 mg/g. Isotherm models for adsorption interaction were investigated deeply, and it was determined that the adsorption mechanism is suitable for Langmuir isotherm.

Keywords: adsorption; estradiol; hydrophobic; L-phenylalanine; microparticle.

***Corresponding author: Kadir Erol,** Hitit University, Vocational School of Health Services, Department of Medical Services and Techniques, 19030 Çorum, Turkey, E-mail: kadirerol86@gmail.com
Osman Kireç, Department of Chemistry, Faculty of Science, Dicle University, 21280 Diyarbakır, Turkey
İhsan Alacabey, Vocational School of Health Services, Mardin Artuklu University, 47200 Mardin, Turkey
Hüseyin Alkan, Department of Biochemistry, Faculty of Pharmacy, Dicle University, 21280 Diyarbakır, Turkey

1 Introduction

Microcontaminants for aquatic life have become an essential global problem in recent years. These compounds consist of many organic compounds from human or natural sources, including paint industries [1, 2], drugs [3–5], heavy metals [6–8], anion [9, 10] and live products, steroid hormones and agrochemicals [11]. Such substances are present in very low concentrations in water, and each has a specific mechanism of action [12]. The removal of pollutants in water systems and making these waters more suitable for the environment and human health is an important issue that the scientific world focuses on and tries to produce new solutions every day [13–18]. Some types of these pollutants called endocrine disruptors (EDs) cause reproductive system deformities, some developmental defects of children and a massive increase in cancer risk [19]. Estradiol (E2 or 17β-estradiol) is one of these EDs, which has been the subject of investigation since the 1930s [18]. E2 is the dominant sex hormone found in women, and it is significant for the growth and preservation of the female reproductive system [20]. As a result, E2 is used worldwide as a vital drug. The global market sales of E2 amounted to approximately 1968 million US $ in 2013 [18]. Thus, E2 regularly pollutes water bodies. It can cause fish egg production to be blocked, males reversed, and even the collapse of local fish populations [21]. Also, E2 has excellent environmental stability, degradation resistance and bioaccumulation tendency. Therefore, it is challenging to remove E2 from traditional drinking and wastewater treatment plants altogether [22]. It is, therefore, vital to develop an optimum method for removing E2 from aqueous environments [23–28].

For this reason, adsorption, which is accepted as the universal method of water treatment, draws attention as an effective, fast and environmentally friendly method for removing E2 from water [22]. In recent years, environmentally friendly materials such as chitosan [29], moringa [30], activated carbon [31] and clay mineral [32] have attracted the attention of researchers for adsorption due to their stability, physical and chemical versatility. However, these adsorbents

have different deficiencies, including limited adsorption ability, high production cost, or low extraction efficiencies. Therefore, it is imperative to develop a suitable adsorbent with excellent adsorption properties, low production cost and good regeneration performance for removal of E2 [33–41].

Different types of interactions, such as hydrophobic (dispersant), dipole-dipole, ionic, are used in adsorption studies. Historically, hydrophobic interaction chromatography (HIC) was first described by Shepard and Tisulius in 1949 [42], using the term "salting out chromatography" and later produced by Hjerten [43]. HIC is widely used in protein separation processes as well as in biopolymer science and ion-exchange chromatography [44]. In these processes, the hydrophobic materials adsorb the hydrophobic solutes in a mobile phase at high ionic intensity, and then the desorption step is realized by decreasing the ionic intensity [45].

In this study, a hydrophobic based approach was utilized for adsorption of E2 from aqueous systems. A monomeric derivative of the L-phenylalanine was used for the hydrophobic character of the adsorbent [46, 47]. As the adsorbent, Poly(2-Hydroxyethyl methacrylate-N-methacryloyl-L-Phenylalanine) [Poly(HEMA–MAPA)] microparticles were synthesized, and the adsorption performance of the microparticles for E2 was investigated. Also, isotherm models for adsorption interaction were examined in detail, and thermodynamic calculations were performed. The use of sub-micron size Poly(HEMA-MAPA) hydrophobic particles in E2 adsorption is a vital alternative to the existing studies on E2 removal in the literature.

2 Materials and methods

2.1 Material

2-Hydroxyethyl methacrylate (HEMA) and ethylene glycol dimethacrylate (EGDMA) were obtained from Fluka A.G. (Buchs, Switzerland) and were removed from the polymerization inhibitors by distillation under low pressure before use. Monomers were kept in the refrigerator at 4 °C until use. L-Phenylalanine, 17β-estradiol, methacryloyl chloride and ammonium persulfate (APS) were purchased from Sigma (St. Louis, MO, USA). Poly(vinyl alcohol) (PVAL; molecular weight: 100,000, 98% hydrolyzed) was obtained from Aldrich (USA). MAPA was synthesized in a laboratory environment. All other chemicals are of analytical purity and were supplied by Merck A.G. (Darmstadt, Germany). The conductivity of pure water used in adsorption experiments is 18.2 MΩ cm.

2.2 Methods

2.2.1 Synthesis of *N*-methacryloyl-L-phenylalanine (MAPA): First, a solution in which 5.0 g of L-phenylalanine and 0.2 g of hydroquinone dissolved in 100 mL of dichloromethane (CH_2Cl_2) was prepared in a beaker. The solution was cooled to 0 °C, and then 12.7 g of triethylamine was added to this solution. In the next step, 5.0 mL of methacroyl chloride was slowly poured onto the solution, and this mixture was stirred in a nitrogen atmosphere with a magnetic stirrer for 2 h at room temperature. After the chemical reaction was over, unreacted methacroyl chloride was removed by extraction using 10% NaOH to increase the purity of the product formed. Then the aqueous phase was evaporated, and the remaining solid was dissolved in ethanol.

2.2.2 Preparation of poly(HEMA-MAPA) microparticles: Microemulsion polymerization was carried out in a closed polymerization reactor (500 mL) in a temperature-controlled system. The monomer phase was created from HEMA (10 mL) and MAPA (1.0 g), and APS (0.25 g) used as the initiator was dissolved in the monomer phase. Sonication was performed in an ultrasonic water bath (Bransonic 2200, England) for 5 min at 200 W to dissolve APS in the polymerization medium completely. Then 4.0 g of poly(vinyl alcohol) mixed with 100 mL of ethanol was added to the polymerization reactor with 100 mL of water. During this process, the reactor was continuously stirred at 500 rpm. In the following step, the reactor was purged with nitrogen gas for 5 min and placed in a water bath. The duration of the polymerization process was determined as 8 h under the nitrogen atmosphere when the reactor temperature reached 70 °C (mixing speed: 500 rpm). After completing the polymerization step, the reaction mixture was cooled to room temperature, and the liquid phase was removed by centrifugation (5000 rpm, 10 min). At the end of this process, pale brown Poly(HEMA-MAPA) microparticles were obtained (Figure 1), and the resulting polymer was centrifuged again in the same conditions in 10 mL ethanol to disperse. Washing with ethanol was repeated three times to remove unpolymerized monomers and other chemicals. Finally, the Poly(HEMA-MAPA) microparticles were stored in 10 mL of distilled water at room temperature.

2.2.3 Characterization studies: The average diameter, particle size distribution, and surface morphology of microparticles were examined using a scanning electron microscope (SEM; QUANTA 400F, FEI, The Netherlands). For this, the pre-dried sample was covered with a thin gold layer and vacuumed before being visualized with SEM. Particle size and distribution were measured using at least 300 particles.

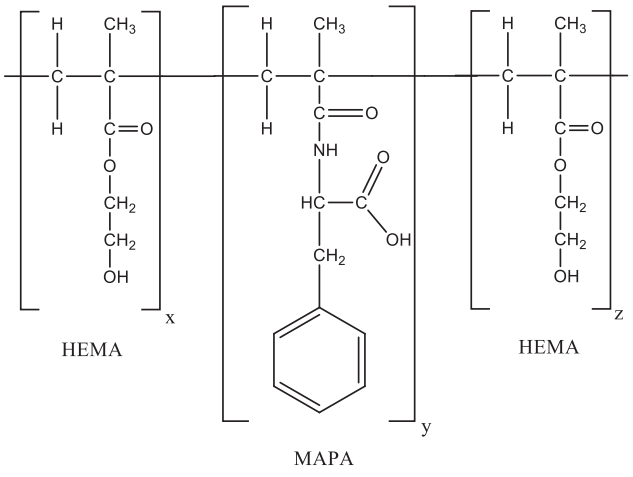

Figure 1: The structure of the poly(HEMA-MAPA).

Fourier transform infrared spectroscopy (FT-IR, 8000 Series, Shimadzu, Japan) was used to determine the specific functional groups of Poly(HEMA-MAPA) microparticles. The FT-IR spectrum was obtained by converting the microparticles into pellets that were homogeneously mixed with dry powder KBr (0.1 g, IR Grade, Merck, Germany).

The amount of incorporation into the Poly(HEMA-MAPA) polymer of the MAPA monomer was determined by the elemental analyzer (Leco, CHNS–932, USA).

In the surface area calculation of Poly(HEMA-MAPA) microparticles, the following equation was used, which gives the number of particles in 1 mL suspension.

$$N = 6 \times 10^{10} \times S/\pi \times \rho_s \times d^3 \quad (1)$$

where N is the number of microparticles in 1 mL suspension; S % solid; d diameter (μm); ρ_s show polymer density. From Equation (1), the specific surface area was calculated in m^2/g unit.

2.2.4 Adsorption–desorption studies: Adsorption of E2 to Poly(HEMA-MAPA) microparticles from aqueous mediums was investigated in the batch system. The particles (0.1 g) were incubated with 50 mL of E2 solution for 2.5 h (equilibrium time) at 150 rpm. The effect of E2 concentration, ionic strength and temperature changes on adsorption capacity was studied. The NaCl concentration was changed between 0.1 and 1.5 M to determine the effect of salt concentration. The concentration values were changed between 5 and 150 mg/mL to research the effect of the initial concentration of E2 on the adsorption capacity. The adsorption works were studied between 4 and 45 °C to investigate the effect of the temperature. Concentrations of 17β-estradiol were determined on the UV–VIS spectrophotometer at a wavelength of 280 nm. The E2 adsorption capacity was calculated by mass balance equation.

$$q = \frac{(C_i - C_f).V}{m} \quad (2)$$

where q is the amount of E2 (mg/g) adsorbed by the particle unit mass; C_i and C_f are concentrations (mg/mL) of E2 initially and after treatment for a particular time; V is the volume of the aqueous solution and m is the mass of the particles used (g). Experimental studies were repeated three times to see the accuracy of the results and calculate the standard deviation.

Desorption of E2 adsorbed from Poly(HEMA-MAPA) is also used in the batch system. The adsorbed particles (50 mg) of E2 were continuously stirred (150 rpm) at room temperature for 2.5 h in 10 mL desorption medium with acetonitrile:methanol (70:30; v:v) solution. Besides, the same particles were subjected to the adsorption/desorption process 10 times to control whether the particles can be used more than once.

3 Results and discussion

3.1 Characterization studies

Poly(HEMA-MAPA) microparticles were produced by microemulsion polymerization in a diameter range of 120–200 nm. An advantage of microparticles is that the contact surface is quite large. Surface morphology and cross-sectional structures of Poly(HEMA-MAPA) microparticles were investigated using SEM. The SEM images of the microparticles are given in Figure 2. As you can see, microparticles are in the form of particles and have smooth surface properties. Also, it is noteworthy that microparticles have a general uniform structure.

FT-IR spectra of Poly(HEMA-MAPA) and MAPA were taken to determine whether the MAPA monomer entered the structure [48]. When Figure 3 is examined, the common bands in both spectra originate from the MAPA monomer are outstanding. These bands are C=C stretching (1500–1600 cm^{-1}), C–N stretching (1180–1360 cm^{-1}), C–H stretching (aromatic, 3010–3100 cm^{-1}), O–H stretching in the carboxylic acid (3500–3600 cm^{-1}), C=O stretching of acid and amide (1690–1760 cm^{-1}), C–O stretching of amide (1657 cm^{-1}), and C–H stretching (2850–2970 cm^{-1}). These results indicate that MAPA entered the structure of the microparticle. Besides, when the spectra are examined, it is seen that these bands are more severe and broader for Poly(HEMA-MAPA) microparticles. The stretching or

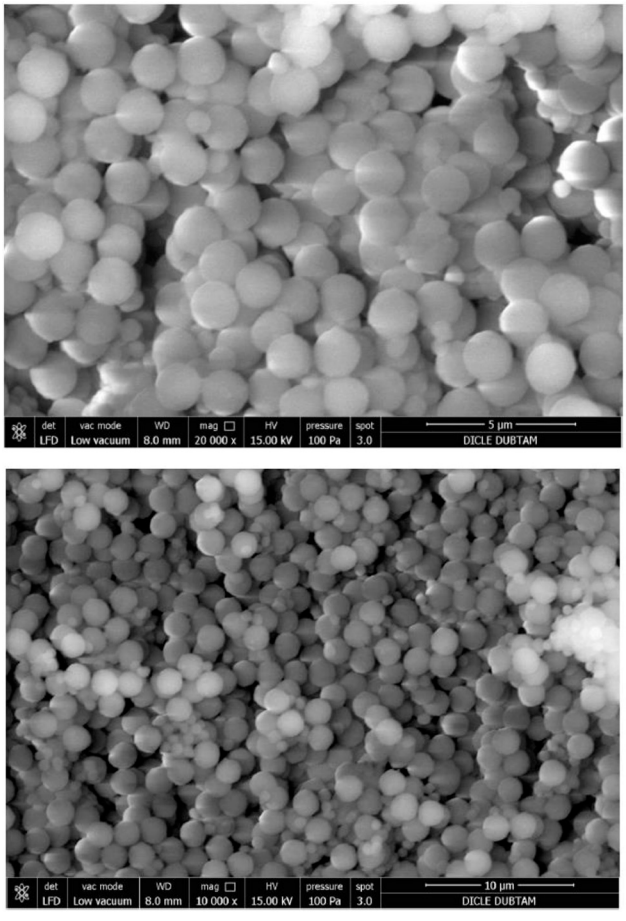

Figure 2: SEM images of poly(HEMA-MAPA) microparticles.

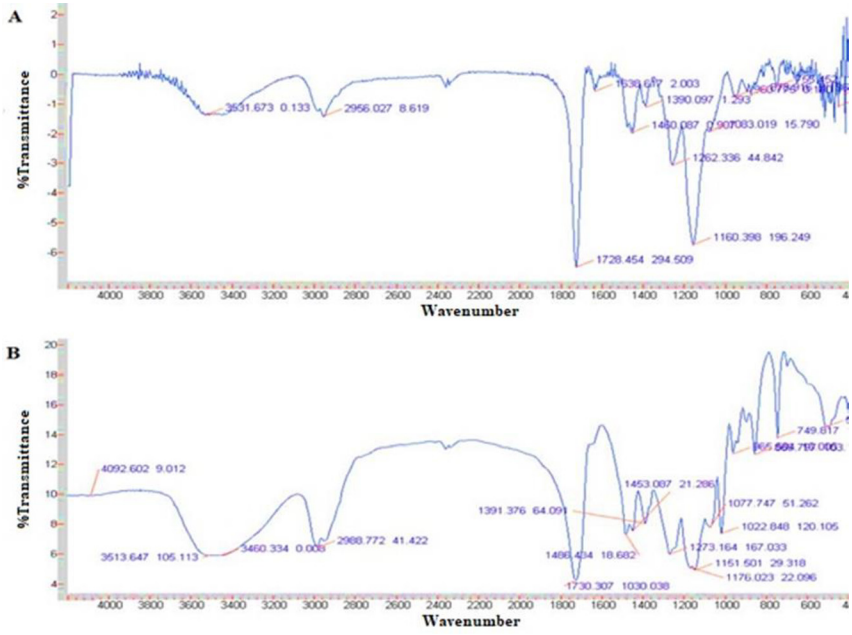

Figure 3: FT-IR spectra of (A) MAPA, (B) poly(HEMA-MAPA) [48].

bending of CO, CH, OH, and -O- groups in HEMA monomers in Poly(HEMA-MAPA) microparticles causes this difference.

It was used with nitrogen stoichiometry to determine the MAPA content of Poly(HEMA-MAPA) microspheres and was calculated as 0.43 mmol/g. Since nitrogen is not found in the structure of the HEMA monomer, this value is an indication that MAPA enters the polymeric structure as desired. The specific surface area of Poly(HEMA-MAPA) microparticles was found to be 1890 m^2/g. This high surface area value appears to be an essential advantage for adsorption interaction.

3.2 Adsorption–desorption studies

To understand the relationship of the initial concentration of E2 with the maximum adsorption capacity, the concentration of E2 was taken at values ranging from 5 to 150 mg/mL. Figure 4 shows the relationship of the initial concentration to the adsorption capacity. The amount of E2 adsorbed in the amount of 1.0 g microparticle first increases with the concentration of the initial E2 and reaches the plateau at a concentration of 100 mg/mL. This is an indication that the active regions of the microparticles fully interact with the E2 in the medium.

In hydrophobic interaction chromatography (HIC), the addition of various salts to the execution and balancing buffer enhances ligand–biomolecule interaction. The ionic strength of the neutral salt added to the medium also affects the solubility of the biomolecules. The ionic strength determines the number and concentration of the cations and anions that make up the salt. The effect of ionic intensity on the adsorption of E2 with Poly(HEMA-MAPA) microparticles was examined in the batch system. The ionic intensity was adjusted with NaCl, and 0.1–1.5 M concentration range was scanned for this salt. The results obtained are presented in Figure 5. As can be seen from the figure, E2 adsorption capacity increased as the salt concentration increased. Because, with increasing salt concentration, the amount of adsorption increases as the diffusion of E2 in the aqueous solution to microparticles increases due to the salting-out of salts. In other words, when a large amount of neutral salt is added to the solution, the water molecules around the hydrophobic groups located in the interior of the biomolecules are removed by

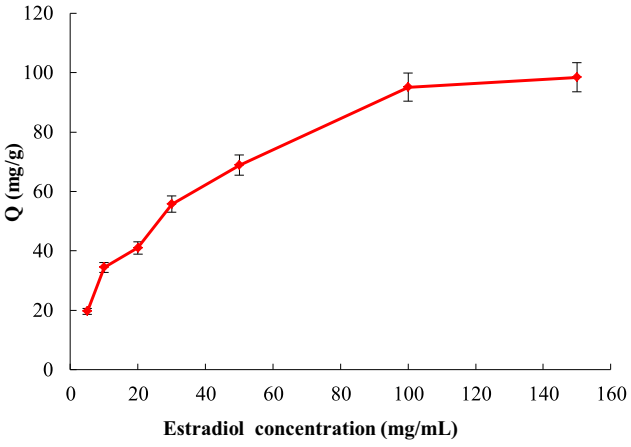

Figure 4: The effect of the starting concentration of 17β-estradiol on adsorption capacity. Interaction time: 2.5 h, temperature: 25 °C.

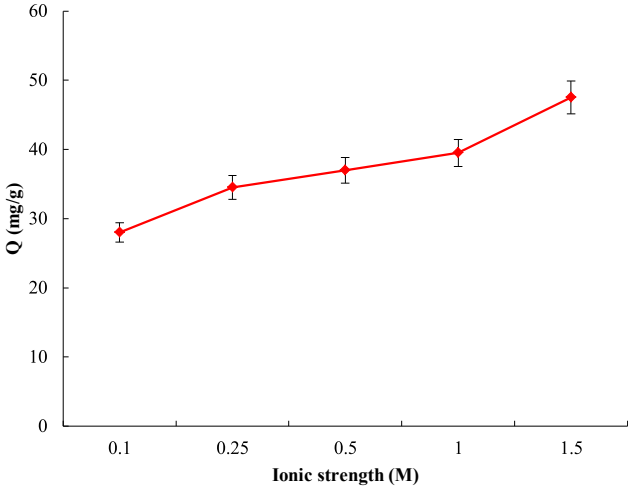

Figure 5: The effect of ionic strength on adsorption capacity. 17β-estradiol concentration: 20 mg/mL, interaction time: 2.5 h, temperature: 25 °C.

the salt ions, in this case, the interaction of the hydrophobic groups with each other increases.

The effect of temperature on the adsorption of E2 was examined in the range of 4–45 °C. As shown in Figure 6, adsorption of E2 on Poly(HEMA-MAPA) increased when the temperature was raised from 4 °C to 45 °C. E2 was adsorbed at 4 and 45 °C in amounts of 23.91 and 42.79 mg/g, respectively. In HIC, increasing the temperature supports the arrest of the biomolecule, and the reduction of the temperature supports the elution of the biomolecule. Indeed, HIC is an entropy-based procedure. Since ΔH can be a small positive or negative value, ΔG is controlled by a positive entropy value. Thus, hydrophobic interaction increases with rising temperature.

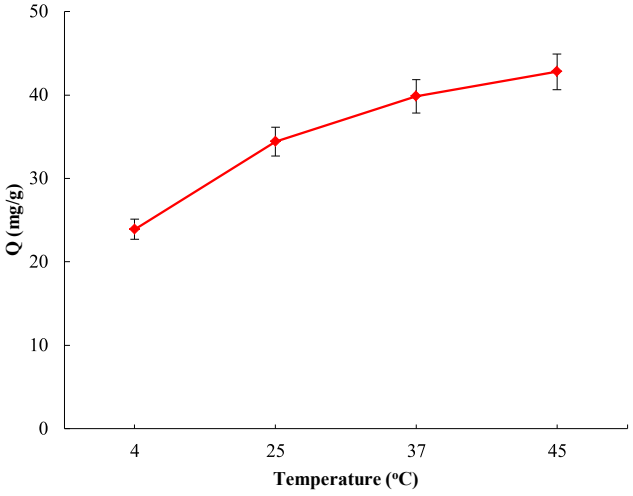

Figure 6: The effect of temperature on adsorption capacity. 17β-estradiol concentration: 20 mg/mL, interaction time: 2.5 h.

E2 adsorbed to microparticles was desorbed in acetonitrile:methanol (70:30, v/v) for 4 h in a batch system (at 150 rpm, at room temperature). The adsorption–desorption process was repeated 10 times using the same microparticles to test the reusability of Poly(HEMA-MAPA) microparticles. Washing was carried out in 2 mM NaOH solution for 30 min to sterilize the microparticles subjected to desorption. After this procedure, the microparticles were washed with distilled water for 30 min. As can be seen from Figure 7, microparticles are very stable, and at the end of 10 repeated adsorption–desorption cycles, there was no appreciable decline in adsorption capacity. In the all adsorption–desorption process of E2, recovery was achieved as 92.7%.

E2 adsorption study was also performed with Poly(HEMA) microparticles to investigate the effect of MAPA in E2 adsorption with Poly(HEMA-MAPA) microspheres. As a result of the study, the adsorption capacity of 2.3 mg/g that is 2.34% of the value achieved by Poly(HEMA-MAPA) was obtained. This result proves to us that the interaction of E2 with the polymeric structure takes place over MAPA. The reason for the small amount of adsorption with Poly(HEMA) microparticles is undesirable non-specific interactions.

3.3 Adsorption isotherms

Adsorption isotherm models; Freundlich, Langmuir (five linearized equations), Temkin, Dubinin–Radushkevich (D-R), Harkins-Jura, Halsey and Frumkin were used to explain the structure of E2 adsorption (surface properties, adsorption mechanism and capacity) with Poly(HEMA-MAPA) microparticles. The equations and parameters of

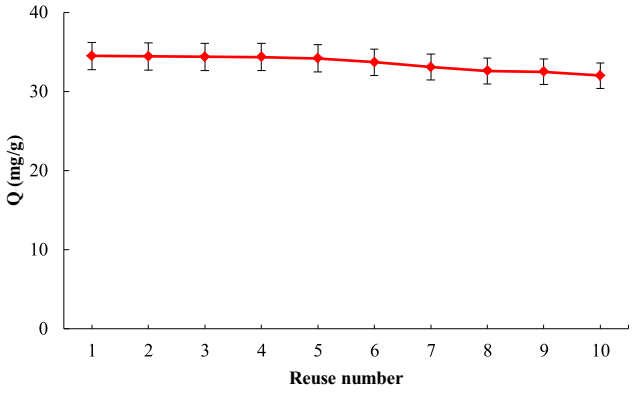

Figure 7: Reusability of poly (HEMA-MAPA) microparticles. 17β-estradiol concentration: 20 mg/mL, interaction time: 2.5 h, temperature: 25 °C.

the isotherm models used are presented in Table 1 with references.

Equations of Langmuir and Freundlich are used to evaluate the balance data of the adsorption process (in the case of two-parameter models). The five equations of the Langmuir isotherm model and the equation of the Freundlich isotherm model were applied to equilibrium data. Langmuir isotherm theory assumes that the adsorbate is monolayer coated on a homogeneous adsorbent surface. According to the Freundlich isotherm, the adsorption sites on the surface of an adsorbent are heterogeneous; that is, they consist of different types of adsorption sites [57].

In Table 2, it was seen that the correlation factors in the five models of Langmuir isotherm were between $0.8724 \le R^2 \le 0.9949$ and that the adsorption structure was compatible with the Langmuir – 2 isotherm ($R^2 = 0.99949$). This result indicates that adsorption takes place in a single layer and is homogeneous.

R_L values indicate that adsorption is negative ($R_L > 1$), linear ($R_L = 1$), appropriate ($0 < R_L < 1$) and irreversible

Table 1: Adsorption isothems.

Isotherm	Linear form	Constants	References
Freundlich	$lnq_e = lnK_F + \frac{1}{n} lnC_e$	K_F (Lmg^{-1}): adsorption capacity. n: heterogeneity factor.	[57]
Langmuir – 1	$\frac{1}{q_e} = \left(\frac{1}{bq_m}\right)\frac{1}{C_e} + \frac{1}{q_m}$	q_m (mgg^{-1}): max adsorption capacity. b (Lmg^{-1}): the constant related to the free energy of adsorption.	[51]
Langmuir – 2	$\frac{C_e}{q_e} = \frac{1}{q_m} C_e + \frac{1}{bq_m}$	q_m (mgg^{-1}): max adsorption capacity. b (Lmg^{-1}): the constant related to the free energy of adsorption.	[51]
Langmuir – 3	$q_e = q_m - \left(\frac{1}{b}\right)\frac{q_e}{C_e}$	q_m (mgg^{-1}): max adsorption capacity. b (Lmg^{-1}): the constant related to the free energy of adsorption.	[51]
Langmuir – 4	$\frac{q_e}{C_e} = bq_m - bq_e$	q_m (mgg^{-1}): max adsorption capacity. b (Lmg^{-1}): the constant related to the free energy of adsorption.	[51]
Langmuir – 5	$\frac{1}{C_e} = bq_m\frac{1}{q_e} - b$	q_m (mgg^{-1}): max adsorption capacity. b (Lmg^{-1}): the constant related to the free energy of adsorption.	[51]
Temkin	$\theta = \frac{RT}{\Delta Q} lnK_o + \frac{RT}{\Delta Q} lnC_e$ $\theta = \left(\frac{q_e}{q_m}\right)$	θ: fractional occupation. q_m (mg g^{-1}): Langmuir-2 max adsorption capacity. The theoretical monolayer saturation capacity. ΔQ: adsorption energy change (kJ/mol.K). K_o: Temkin equilibrium constant (L mg^{-1}). T (K): absolute temperature. R: universal gas constant (8.314 JK^{-1} mol^{-1}).	[50, 51, 58]
Dubinin–Radushkevich	$\ln q_e = \ln q_m - \beta\varepsilon^2$. $\epsilon = RTln\left[1 + \frac{1}{C_e}\right] E_a = \left[\frac{1}{\sqrt{2\beta}}\right]$	q_m (mgg^{-1}): D–R adsorption capacity. β (mol^{2}kJ^{-2}): adsorption average free energy coefficient. ε (kJ^2/mol^2): polanyi adsorption potential. E_a (kJmol^{-1}): D–R adsorption free energy. R: universal gas constant (8.314 JK^{-1}mol^{-1}) and T (K) absolute temperature.	[59]
Halsey	$\frac{1}{q_e} = \frac{1}{n} lnk - \frac{1}{n} lnC_e$	k and n isotherm constants	[54]
Frumkin	$\ln\left[\left(\frac{\theta}{1-\theta}\right)\frac{1}{C_e}\right] = lnk + 2a\theta\theta = \left(\frac{q_e}{q_m}\right) lnk = -\frac{\Delta G}{RT}$	θ: fractional occupation. a: the interaction coefficient. k: related to adsorption equilibrium. q_m (mg g^{-1}): Langmuir-2 max adsorption capacity. G: Gibbs free energy. R: universal gas constant 8.314 JK^{-1}mol^{-1} and T (K) absolute temperature.	[53]
Harkins – Jura	$\frac{1}{q_e^2} = \frac{B_{HJ}}{A_{HJ}} - \frac{1}{A_{HJ}} \log C_e$	B_{HJ} and A_{HJ} are the isotherm constants	[60]

Table 2: Adsorption isotherm values and correlation coefficients (298 K).

		b (L/mg)	q_m (mg/g)	R^2	Temkin		K_o (L/mg)	ΔQ (kJ/mol.K)	R^2
Langmuir	Type 1	0.2707	2.8314	0.9613			1.1789	5.0635	0.9273
	Type 2	0.2411	2.8737	0.9949	Harkins–Jura		A_{HJ}	B_{HJ}	R^2
	Type 3	0.3036	2.7543	0.8724			36.7673	1.7077	0.7449
	Type 4	0.2648	2.8554	0.8724	Halsey		n	k	R^2
	Type 5	0.2551	2.8885	0.9613			3.7351	1.0530	0.8751
Freundlich	n	$1/n$	K_F mg/g)	R^2	Frumkin	a	k	ΔG	R^2
	3.7351	0.2677	1.0139	0.8751		−3.2948	3.5292	−3.1244	0.9381
Dubinin–Radushkevich		q_m (mol/g)	E_a (KJ/mol)	R^2					
		2.4028	0.6484	0.9434					

($R_L = 0$) [57]. As shown in Table 3, R_L values are suitable because they are in the range of $0 < R_L < 1$.

$$R_L = \frac{1}{1 + K_L C_0} \tag{3}$$

Temkin adsorption model is an adsorption isotherm showing the indirect effects of adsorbent–adsorbate interactions on adsorption. According to Temkin isotherm, the heat of adsorption of all molecules in the layer decreases linearly [50]. Surface coverage value (θ) is calculated using the maximum adsorption capacities (q_m) determined in the Langmuir and Freundlich models. Parameters and correlation coefficient of Temkin model are given in Table 2. The very higher values of the correlation coefficient show good linearity whatever the maximum adsorption capacity used for the calculation of surface coverage [51].

As seen in Table 2, the change value (ΔQ) of the adsorption energy is 5.064 kJ mol^{-1}. A positive value $\Delta Q = (-\Delta H)$ indicates that the adsorption reaction is exothermic. The adsorption energy change (ΔQ) calculated from the Temkin isotherm equation shows that the adsorption is realized by physical interactions when $0 < \Delta Q < 100$ [50].

According to the Dubinin–Radushkevich isotherm theory, sorption energy E ($kJmol^{-1}$) gives information about the physical and chemical properties of adsorption. E value below 8.0 $kJmol^{-1}$ means that the sorption process takes place through the physical mechanism [52]. Since the E value calculated in Table 2 is below 8.0 $kJmol^{-1}$ (0.6484 $kJmol^{-1}$), the mechanism of E2 adsorption on the Poly(HEMA-MAPA) microparticles is physical.

Frumkin isotherm takes into account the interaction between adsorbed species [53]. In Table 2, the ΔG value for E2 adsorption was calculated as −31,244 $kJmol^{-1}$. This result shows that the adsorption process is spontaneous.

The Halsey equation is suitable for multilayered adsorption and can be attributed to the heterosporous nature of the adsorbent [54]. Like the Freundlich isotherm, the Halsey model is also suitable for multilayer adsorption [55]. The Harkins–Jura isotherm describes multilayered adsorption and can be explained by the presence of a heterogeneous pore distribution [56].

As a result, it was found that the adsorption mechanism has a single layer and homogeneous surface. Additionally, the adsorption process takes place spontaneously through the physical mechanism, and the adsorption reaction is exothermic.

Table 3: R_L values for Langmuir −2 isotherm.

C_0 (mg/L)	298 K
	R_L
5	0.4534
10	0.2932
20	0.1718
30	0.1215
50	0.0766

4 Conclusion

At this work, thanks to the phenylalanine contained in MAPA, the polymeric structure has a hydrophobic character. Since the target molecule E2 is also hydrophobic in structure, hydrophobic interaction chromatography was chosen as the appropriate method for adsorption studies. Since the amount of adsorption increased with increasing temperature and ionic intensity, the interaction between adsorbent and adsorbate was confirmed by hydrophobic basis. Adsorption mechanism found in accordance with the Langmuir isotherm model. In other words, adsorption was homogeneous and monolayer. It was determined that the adsorption interaction occurred spontaneously and

physically. As a result, it can be said that Poly(HEMA-MAPA) microparticles are suitable materials for E2 adsorption from aqueous solutions.

Acknowledgments: All the authors of this study would like to express their gratitude to Prof. Dr. Adil Denizli (Hacettepe University) for his valuable contribution.
Author contributions: All the authors have accepted responsibility for the entire content of this submitted manuscript and approved submission.
Research funding: None declared.
Conflict of interest statement: The authors declare no conflicts of interest regarding this article.

References

1. Erol K., Köse K., Köse D. A., Sızır Ü., Tosun Satır İ., Uzun L. *Desalination Water Treat.* 2016, *57*, 9307–9317.
2. García J. R., Sedran U., Zaini M. A. A., Zakaria Z. A. *Environ. Sci. Pollut. Control Ser.* 2018, *25*, 5076–5085.
3. Gong H., Chu W. *Ind. Eng. Chem. Res.* 2015, *54*, 12763–12769.
4. Quesada H. B., Baptista A. T. A., Cusioli L. F., Seibert D., de Oliveira Bezerra C., Bergamasco R. *Chemosphere* 2019, *222*, 766–780.
5. Lin A. Y. C., Hsueh J. H. F., Hong P. A. *Environ. Sci. Pollut. Control Ser.* 2015, *22*, 508–515.
6. Abbas K., Znad H., Awual M. R. *Chem. Eng. J.* 2018, *334*, 432–443.
7. Awual M. R., Hasan M. M., Znad H. *Chem. Eng. J.* 2015, *259*, 611–619.
8. Bilgin E., Erol K., Köse K., Köse D. A. *Environ. Sci. Pollut. Control Ser.* 2018, *25*, 27614–27627.
9. Singh S., German M., Chaudhari S., Sengupta A. K. *J. Environ. Manag.* 2020, *263*, 110415.
10. Xu X., Gao B., Jin B., Yue Q. *J. Mol. Liq.* 2016, *215*, 565–595.
11. Erol K., Yıldız E., Alacabey İ., Karabörk M., Uzun L. *Environ. Sci. Pollut. Control Ser.* 2019, *26*, 33631–33641.
12. Li L., Iqbal J., Zhu Y., Wang F., Zhang F., Chen W., Wu T., Du Y. *Int. J. Biol. Macromol.* 2020, *145*, 686–693.
13. Basheer A. A. *Chirality* 2018, *30*, 402–406.
14. Basheer A. A., Ali I. *Chirality* 2018, *30*, 1088–1095.
15. Basheer A. A. *J. Mol. Liq.* 2018, *261*, 583–593.
16. Ali I., Jain C. *Curr. Sci.* 1998, *75*, 1011–1014.
17. Ali I., Gupta V. K., Aboul-Enein H. Y. *Electrophoresis* 2005, *26*, 3988–4002.
18. Ali I., Alothman Z. A., Alwarthan A. *J. Mol. Liq.* 2017, *241*, 123–129.
19. Koç İ., Baydemir G., Bayram E., Yavuz H., Denizli A. *J. Hazard Mater.* 2011, *192*, 1819–1826.
20. Ryan K. J. *Cancer. Res.* 1982, *42*, 3342s–3344s.
21. Jiang L., Liu Y., Zeng G., Liu S., Hu X., Zhou L., Tan X., Liu N., Li M., Wen J. *Chem. Eng. J.* 2018, *339*, 296–302.
22. Liu S., Li M., Liu Y., Liu N., Tan X., Jiang L., Wen J., Hu X., Yin Z. *J. Taiwan Inst. Chem. Eng.* 2019, *102*, 330–339.
23. Li L., Long Y., Chen Y., Wang S., Wang L., Zhang S., Jiang F. *Solid State Sci.* 2018, *83*, 143–151.
24. Ali I., Alharbi O. M., ALOthman Z. A., Al-Mohaimeed A. M., Alwarthan A. *Environ. Res.* 2019, *170*, 389–397.
25. Nodeh H. R., Ibrahim W. A. W., Ali I., Sanagi M. M. *Environ. Sci. Pollut. Control Ser.* 2016, *23*, 9759–9773.
26. Burakova E. A., Dyachkova T. P., Rukhov A. V., Tugolukov E. N., Galunin E. V., Tkachev A. G., Ali I. *J. Mol. Liq.* 2018, *253*, 340–346.
27. Ali I., Mbianda X., Burakov A., Galunin E., Burakova I., Mkrtchyan E., Tkachev A., Grachev V. *Environ. Int.* 2019, *127*, 160–180.
28. Ali I. *J. Mol. Liq.* 2018, *271*, 677–685.
29. Subedi N., Lähde A., Abu-Danso E., Iqbal J., Bhatnagar A. *Int. J. Biol. Macromol.* 2019, *137*, 948–959.
30. Shirani Z., Santhosh C., Iqbal J., Bhatnagar A. *J. Environ. Manag.* 2018, *227*, 95–106.
31. Iqbal J., Shah N. S., Sayed M., Imran M., Muhammad N., Howari F. M., Alkhoori S. A., Khan J. A., Khan Z. U. H., Bhatnagar A. *J. Clean. Prod.* 2019, *235*, 875–886.
32. Maged A., Iqbal J., Kharbish S., Ismael I. S., Bhatnagar A. *J. Hazard Mater.* 2020, *384*, 121320.
33. Ali I., Aboul-Enein H. Y. *Crit. Rev. Anal. Chem.* 2002, *32*, 337–350.
34. Ali I., Alharbi O. M., Tkachev A., Galunin E., Burakov A., Grachev V. A. *Environ. Sci. Pollut. Control Ser.* 2018, *25*, 7315–7329.
35. Ali I., Alharbi O. M., Alothman Z. A., Alwarthan A. *Colloids Surf. B Biointerfaces* 2018, *171*, 606–613.
36. Ali I., Alharbi O. M., Alothman Z. A., Badjah A. Y. *Photochem. Photobiol.* 2018, *94*, 935–941.
37. Ali I., Alharbi O. M., ALOthman Z. A., Alwarthan A., Al-Mohaimeed A. M. *Int. J. Biol. Macromol.* 2019, *132*, 244–253.
38. Ali I., Burakov A. E., Melezhik A. V., Babkin A. V., Burakova I. V., Neskomornaya M. E. A., Galunin E. V., Tkachev A. G., Kuznetsov D. V. *Chemistry Select* 2019, *4*, 12708–12718.
39. Al-Shaalan N. H., Ali I., ALOthman Z. A., Al-Wahaibi L. H., Alabdulmonem H. *J. Mol. Liq.* 2019, *289*, 111039.
40. Ali I., Khan T. A., Hussain I. *Int. J. Environ. Eng.* 2011, *3*, 48–71.
41. Ali I., Aboul-Enein H. Y. *Chemosphere* 2002, *48*, 275–278.
42. Shepard C. C., Tiselius A. *Chromatographic Analysis*; Discusions of the Faraday Society, Hazell, Watson and Winey: London, 1949.
43. Hjertén S. *J. Chromatogr. A* 1973, *87*, 325–331.
44. Galeotti N., Hackemann E., Jirasek F., Hasse H. *Separ. Purif. Technol.* 2020, *233*, 116006.
45. Zhang L., Wu S. *J. Chromatogr. A* 2020, *1611*, 460576.
46. Saylan Y., Sarı M. M., Özkara S., Uzun L., Denizli A. *Mater. Sci. Eng. C* 2012, *32*, 937–944.
47. Uygun D. A., Karagözler A. A., Akgöl S., Denizli A. *Mater. Sci. Eng. C* 2009, *29*, 2165–2173.
48. Türkmen D., Öztürk N., Akgöl S., Elkak A., Denizli A. *Biotechnol. Prog.* 2008, *24*, 1297–1303.
49. Gökırmak-Söğüt E., Caliskan N. *Fresenius Environ. Bull.* 2017, *26*, 2720–2728.
50. Işıkver Y. *Cumhuriyet Sci. J.* 2017, *38*, 770–780.
51. Hamdaoui O., Naffrechoux E. *J. Hazard Mater.* 2007, *147*, 381–394.
52. Caliskan N., Kul A. R., Alkan S., Sogut E. G., Alacabey I. *J. Hazard Mater.* 2011, *193*, 27–36.
53. Sarıcı-Özdemir Ç., Önal Y., Erdoğan S., Akmil-Başar C. *Fresenius Environ. Bull.* 2012, *21*, 84–93.
54. Riza K. A., Tolga D., Ihsan A., Salih A., Yunus O. *Fresenius Environ. Bull.* 2011, *20*, 1155–1166.

55. Chen J. P., Wang L. K., Wang M. H. S., Hung Y. T., Shammas N. K. *Remediation of Heavy Metals in the Environment*; CRC Press: Florida, 2016.
56. Vargas A. M., Cazetta A. L., Kunita M. H., Silva T. L., Almeida V. C. *Chem. Eng. J.* 2011, *168*, 722–730.
57. Acet Ö., Baran T., Erdönmez D., Aksoy N. H., Alacabey İ., Menteş A., Odabaşi M. *J. Chromatogr. A* 2018, *1550*, 21–27.
58. Wang Y., Xie Y., Zhang Y., Tang S., Guo C., Wu J., Lau R. *Chem. Eng. Res. Des.* 2016, *114*, 258–267.
59. Wakkel M., Khiari B., Zagrouba F. *Environ. Sci. Pollut. Control Ser.* 2019, *26*, 18942–18960.
60. Ponnuchamy M., Kapoor A., Pakkirisamy B., Sivaraman P., Ramasamy K. *Environ. Sci. Pollut. Control Ser.* 2019, 1–22.